Published in final edited form as:
Neuron. 2008 August 14; 59(3): 462–474. doi:10.1016/j.neuron.2008.06.011.

Mouse Cone Photoreceptors Co-express Two Functional Visual Arrestins

Sergei S. Nikonov[1], **Bruce M. Brown**[2], **Jason A. Davis**[1], **Freddi I. Zuniga**[2], **Alvina Bragin**[1], **Edward N. Pugh Jr.**[1], and **Cheryl M. Craft**[2,3]

1*F. M. Kirby Center for Molecular Ophthalmology, Department of Ophthalmology, School of Medicine, University of Pennsylvania*

2*Mary D. Allen Laboratory for Vision Research, Doheny Eye Institute, Department of Ophthalmology, Keck School of Medicine, University of Southern California*

3*Department of Cell & Neurobiology, Keck School of Medicine, University of Southern California*

Abstract

Arrestins are members of a superfamily of proteins that arrest the activity of G-protein coupled receptors. Mouse cone photoreceptors express two visual arrestins, Arr1 and Arr4 (Carr). We quantified their expression levels and subcellular distributions in mouse cones: total Arr1 was estimated to be in an ~ 6:1 ratio to cone opsin, about 50-fold higher than Arr4. Recordings from single cones of *Arr1*$^{-/-}$ and *Arr4*$^{-/-}$ mice establish that both proteins are competent to arrest the activity of photoactivated S- and M- cone opsins. Recordings from *Arr1*$^{-/-}$, *Arr4*$^{-/-}$ double-knockout mice establish a requirement for at least one of the two visual arrestins for normal cone opsin inactivation at all flash intensities. These recordings also reveal low activity photoproducts of S- and M-opsins that are absent when Grk1 and an arrestin are co-expressed, but which decay 70-fold more rapidly than the comparable photoproducts of rhodopsin in rods.

INTRODUCTION

Arrestins arrest the activity of G-protein coupled receptors (GPCRs) after they are phosphorylated by G-protein receptor kinases (GRKs) (Gurevich and Gurevich, 2006a;Gurevich and Gurevich, 2006b). Arrestin 1 (ARR1) was the first member of the family to be discovered and was established in the 1980's to inhibit the activation of transducin by photoactivated rhodopsin, after the latter is phosphorylated by rhodopsin kinase (GRK1) (Kuhn et al., 1984;Wilden et al., 1986). The requirement for GRK1 and ARR1 in the normal inactivation of rod photoresponses, including those to single photons, was established definitively in experiments with rods of *Grk1*$^{-/-}$ (Chen et al., 1999a) and *Arr1*$^{-/-}$ mice (Xu et al., 1997).

Correspondence regarding animals and molecular biology to: Professor Cheryl M. Craft, Ph.D., Departments of Ophthalmology, and Cell & Neurobiology, Keck School of Medicine, University of Southern California, 1355 San Pablo Street, DVRC 405, Los Angeles, CA 90033-9224. *Correspondence regarding electrophysiology and quantitation to:* Professor Edward N. Pugh, Jr, Ph.D., Department of Ophthalmology, F.M. Kirby Center for Molecular Ophthalmology, Stellar-Chance Building, Room 309B, 422 Curie Boulevard, Philadelphia, PA 19104-6069.

Craft et al. (1994) discovered that all cone photoreceptors and a subset of pinealocytes express a novel visual arrestin, CARR (hereafter, ARR4) distinct from ARR1 (see Methods, "Nomenclature"). It is reasonable to hypothesize that the normal downregulation of cone opsin signaling requires phosphorylation by a GRK and subsequent binding of ARR4, in homology with the GRK1- and ARR1-dependent inactivation of rhodopsin in rods. In support of this hypothesis (Zhu et al., 2003) found that mouse cone S- and M-opsins illuminated *in vivo* were indeed phosphorylated and bound Arr4 and that in the absence of Grk1 (the only GRK expressed in mouse cone photoreceptors), neither phosphorylation of cone opsins nor Arr4 binding was detectable. The requirement for Grk1 for normal mouse cone inactivation was initially established with paired-flash electroretinographic recordings (Lyubarsky et al., 2000), and later confirmed with recordings of mouse S- and M-opsin photoresponses of single cones of the $Nrl^{-/-}$ mouse (Nikonov et al., 2005). In contrast, the requirement for Arr4 in normal cone opsin shutoff has seemed doubtful (Shi et al., 2007), due in part to a reportedly very low expression level (~1:500 relative to cone opsin) (Chan et al., 2007), and no direct test of the role of Arr4 in the light response of living cones has been reported.

To carry out a definitive test of the hypothesis that ARR4 can function in the inactivation of photoactivated cone opsins, we generated an $Arr4^{-/-}$ mouse and compared the light responses of its cones with those of wildtype (WT) mice. An unexpected complexity developed with the discovery that mouse cones express not only Arr4, but also Arr1 (Zhu et al., 2005). We thus also bred $Arr4^{-/-}$ mice into the $Arr1^{-/-}$ background, and recorded and compared light responses of single cones of mice of the four genotypes: WT, single knockouts $Arr4^{-/-}$, $Arr1^{-/-}$, and $Arr4^{-/-}$ $Arr1^{-/-}$, arrestin double-knockouts (hereafter, "*Arr*-DKO"). Furthermore, because Arr4 in cones, like Arr1 in rods, is widely distributed throughout the cell, and is known to undergo light-dependent redistribution between inner segment and outer segment compartments (Zhu et al., 2002), we quantified the expression levels and subcellular distributions of both visual arrestins in dark adapted mouse cones.

RESULTS

Generation and confirmation of $Arr4^{-/-}$ mice

The strategy used to create mice null for expression of mouse cone arrestin ($Arr4^{-/-}$) is schematized in Figure 1, along with evidence confirming the absence of Arr4 protein product. Homologous recombination of the targeting vector with the WT gene in mouse ES cells replaced exons 1 through 5 with the *LacZ/Neo* cassette. Since all cDNAs encoding *Arr4* isoforms have the same translation start ATG codon (Zhu et al., 2002), this strategy resulted in the knockout of all *Arr4* isoforms, as confirmed by restriction analysis (Supplement), by immunoblot analysis (Fig. 1B) and immunohistochemistry (Fig. 1C; Fig. 2)

Arr4 and Arr1 are both expressed in mouse cones

Mouse retinas express two distinct visual arrestins, Arr4 ("cone arrestin") and Arr1 ("rod arrestin") (Fig. 2), and preliminary evidence has suggested both to be expressed in cones (Zhu et al., 2005). As Arr1 and Arr4 are highly homologous, a prerequisite to establishing their co-expression in cones is the availability of antibodies that can discriminate between them. The antibodies LUMIj and D9F2, raised against unique peptides of Arr4 and Arr1,respectively (Supplement), meet the critical test provided by immunohistochemical labeling of retinal sections of mice of the four genotypes, WT, $Arr4^{-/-}$, $Arr1^{-/-}$, and *Arr*-DKO (Fig. 2). Thus, LUMIj reacts immunochemically only with cones of genotypes that express Arr4 (WT, $Arr1^{-/-}$), while D9F2 reacts only with cones of genotypes that express Arr1 (WT, $Arr4^{-/-}$). Moreover, neither antibody reacts with retinas of *Arr*-DKO mice. While the specificity of LUMIj and D9F2 for Arr4 and Arr1, respectively, is a necessary condition for establishing Arr1 co-expression in cones, additional hurdles remain to be overcome. Arr1 is highly

expressed in rods whose 30 to 1 preponderance over cones and high density in the retina contribute immunofluorescence that may be misinterpreted as originating in cones. To obviate this potential artifact, we employed high resolution, two-color confocal imaging (Fig. 2), which allowed us to probe for Arr1 and Arr4 expression in volume elements (voxels) that lie securely within the boundaries of most segments of the cone.

Determination of the quantities and distributions of Arr1 and Arr4 in cones

Arr4 and Arr1 are distributed throughout the dark adapted photoreceptor layer (Fig. 2), and so we determined their distributions and quantities in the different subcellular compartments of cones.

The ratio of Arr4 to rhodopsin in the mouse retina was estimated with quantitative immunoblot analysis to be ~ 1:550 (Supplement Table S1). Given that a C57Bl/6 eye has 600 pmol rhodopsin (Lyubarsky et al., 2004), and ~ 200,000 cones (Carter-Dawson and LaVail, 1979;Jeon et al., 1998), each retina contains ~ 1.1 pmol Arr4, or 3.3×10^6 molecules/cone. Since each mouse cone outer segment contains ~ 2.7×10^7 opsin molecules (Nikonov et al., 2006), Arr4 stands in a 1:8 ratio to the opsin content of a cone.

The quantity of Arr1 per cone was estimated to be ~ 1.7×10^8 molecules/cone, about 50-fold higher than the quantity of Arr4. This number was obtained by quantitative analysis of the immunofluorescence distribution of the Arr1-specific antibody D9F2 in adjacent rods and cones (Fig. 3; Supplement), combined with a previous estimate of the ratio of Arr1 to rhodopsin in the retina (0.78:1) (Strissel et al., 2006).

The distributions of the two arrestins over the various cone compartments are somewhat different. In particular, Arr4 appears more concentrated in the cone pedicle than is Arr1. (Table 1). The dark adapted cone outer segment contains about 10% of the total Arr1 or Arr4, and so the total quantity of arrestins (predominantly Arr1) in the dark adapted outer segment is about 70% of the quantity of cone opsin.

The activation phase of phototransduction is similar in S-dominant cones lacking one or both visual arrestins

Given that both Arr1 and Arr4 are expressed in mouse cones, it is natural to inquire whether both arrestins function in the downregulation of cone phototransduction. This issue was addressed by comparing the light responses of cones of mice expressing only Arr1 or only Arr4 with responses of WT cones and of cones of mice lacking both arrestins (Fig. 4). Response families of cones of WT, *Arr4*$^{-/-}$ and *Arr1*$^{-/-}$ mice were grossly similar, while those of *Arr*-DKO mice exhibited greatly slowed recovery from strong flashes, considered further below (Fig. 4A, D, G, J). Analysis of the activation phase of the light responses reveals that the amplification constant (*A*) of phototransduction is similar across all four genotypes (Fig. 4B, E, H, K; Table 2). Nonetheless, the average value of *A*for WT cones (4.7 s^{-2}) is reliably lower by 17% than the grand average (5.7 s^{-2}) over all 60 cones, while the average values for cones of the knockout genotypes range from 5% (*Arr1*-DKO) to 23% (*Arr1*$^{-/-}$) above (Table 2). Flash sensitivity ($\tilde{S}_F$) also is reliably different amongst genotypes, such that the mean sensitivity of WT cones is 19% below the grand average, while the mean sensitivities of knockout cone populations range from 4% below average (*Arr4*$^{-/-}$) to 28% above (*Arr1*$^{-/-}$, *Arr1*-DKO) (Table 2). These differences amongst cones of different genotypes in properties characterizing “activation” are modest, however, and support the general conclusion that the initial reactions in cone phototransduction are essentially normal in the knockouts and do not contribute a distinguishing phenotype. It is notable in this context that there are no reliable differences amongst cones in the time to peak (t_{peak}) of the dim-flash response.

Cones lacking Arr1 and Arr4 have slowed initial recovery to strong flashes

A clear phenotype in arrestin knockout mice can be seen in comparison of the initial recoveries of responses of cones of the different genotypes from strong, i.e., saturating, flashes (compare Fig. 4A, D, G, J). This phenotype can be quantified by "Pepperberg plot" analysis, in which the time to reach a criterion level of recovery is plotted semilogarithmically as a function of flash intensity (e.g., 40%, as in Fig.4C, F, I, L) (Pepperberg et al., 1992). A more complete quantification is obtained by plotting the average recovery times of a population of cones of each genotype for several different recovery levels: over the range of saturating intensities, the recovery times of WT^{-}cones are approximately linear in semilog coordinates, with slopes almost independent of the recovery level (Fig. 5; inset). Such recoveries thus obey the "recovery shape invariance" criterion necessary for being well characterized by a dominant time constant, τ_D (Nikonov *et al.*, 1998). For cones lacking Arr1 or Arr4, recovery times deviate slightly from linearity, but again, as for WT cones, are nearly constant with criterion level (Fig. 5, inset). However, in the case of the *Arr*-DKO cones, the variation in slope with criterion is extreme. These analyses confirm for populations of cones what is seen in the records of individual cones in Fig. 4: the expression of *either* Arr1 or Arr4 is sufficient for a relatively normal initial recovery, while the absence of *both* arrestins results in greatly slowed recovery for saturating flashes. Nonetheless, the reliably higher average value of τ_D (~ 85 ms) of *Arr4*$^{-/-}$ and *Arr1*$^{-/-}$ cones over WT cones (63 ms) (Table 2) indicates that the initial phase of recovery from saturating flashes is to some extent slowed by deletion of either arrestin.

Increased amplitude of the "slow tails" of recovery in *Arr*-DKO cones

In WT cones, the initial rapid phase of recovery from saturating flashes is, for the strongest flashes, followed by a second phase, a "slow tail" that increases in amplitude with flash strength (Fig. 4A). In *Arr*-DKO cones the greatly slowed recoveries from saturating flashes do not exhibit two distinct recovery phases, but slow tails are observed in the responses of *Arr4*$^{-/-}$; and *Arr1*$^{-/-}$ cones (Fig. 4D, G), and the amplitude of these tails (at a given flash strength) appears increased in the *Arr1*$^{-/-}$ cones relative to WT and *Arr4*$^{-/-}$ cones. We will return to this matter later, after examining other features of the light responses.

S- and M-cone opsin driven dim-flash responses of cones lacking *both* Arr1 and Arr4 have a slow tail in recovery

It is important to ascertain whether the phenotype seen in the responses of cones lacking visual arrestins to strong light flashes is also present in the "dim-flash" regime. A dim-flash response is one that is linear in flash intensity: linearity is usually taken to imply that with such stimulation the reactions of the phototransduction cascade driven by each photopigment molecule isomerized are identical. Because most mouse cones co-express two cone opsins which have widely separated UV and mid-wave absorbance maxima, dim-flashes of 360 nm and 510 nm light independently probe the time course of phototransduction activated by S- and M-cone opsins, respectively (Nikonov et al., 2006). Consideration of such dim-flash responses of populations of cones of each genotype (Fig. 6) reveals the following. First, for *WT*, *Arr4*$^{-/-}$ and *Arr1*$^{-/-}$ cones, S- and M-opsin driven responses are indistinguishable from each other, both within and across genotypes. Second, *Arr*-DKO cones exhibit a nearly identical response waveform to that of the cones of the other genotypes until they achieve approximately 60% of their recovery to baseline; at this point the recoveries of the *Arr*-DKO cones "peel off", exhibiting a much slower tail phase than do the others. This slowed tail is the same, regardless of whether S- or M-opsin was activated by the flash. From these observations, we conclude that the normal inactivation of each isomerized S- or M-opsin molecule requires at least one of the visual arrestins. Shi et al. (2007) previously reported that the M-opsin driven dim-flash response of cones of *Arr1*$^{-/-}$ mice is not different from that of WT, and our data confirm their observation (Fig. 6, *Arr1*$^{-/-}$). However, a definitive interpretation of this lack of phenotype

could only be made in the context of proof that Arr1 is expressed in cones by a comparison of responses of the *Arr4*$^{-/-}$ cones with those of *Arr*-DKO cones: this comparison now reveals that *Arr4* arrests the activity of cone opsins in the absence of Arr1.

Arrestins contribute to the avoidance of saturation in steady illumination

The slowed recovery of cones null for both arrestins (Fig. 4J; Table 2) implies that the phosphodiesterase activity generated by each photoisomerized cone opsin is prolonged. This prolonged activity should make a cone without arrestins more susceptible to saturation. To test this prediction, we measured the responses of cones of the four genotypes to steps of light and analyzed their dependence on light intensity (Fig. 7). As expected, the step-response amplitude vs. intensity function of *Arr*-DKO cones is shifted to ~ 3-fold lower intensities, and lesser shifts were observed for cones of each of the single knockout genotypes (Fig. 7); these shifts are highly reliable (Table 2). A caveat is called for, however, because both the length of the experiments and requirement of long stability (see Supplement Fig. 9S), made it difficult in some cases (e.g., Fig. 7E, F) to suppress large fractions of the cone circulating current. It is nonetheless clear that the Arr-DKO cones approach saturation at lower light levels than the cones of the other genotypes.

DISCUSSION

Orthologues of ARR4 have been found to be expressed in the cones of all vertebrate species that have been examined, including human (Craft et al., 1994), but prior to this investigation a function for ARR4 had not been established in living cones. A surprising feature of native mouse cones that had to be considered was the possible co-expression in cones of Arr1 (Zhu et al., 2005).

Mouse cones co-express two distinct visual arrestins, Arr4 and Arr1

By immunohistochemical analysis of retinas of WT, *Arr4*$^{-/-}$, *Arr1-4*$^{-/-}$ and *Arr*-DKO mice, we established the specificity of the antibodies D9F2 and LUMIj for Arr1 and Arr4, respectively (Fig. 2), and using high resolution, two-color confocal microscopy with them established that Arr1 and Arr4 are co-expressed in mouse cones (Fig. 3; Supplement). The functional co-expression in individual cones of distinct isoforms of phototransduction proteins, including opsins (Nikonov et al., 2006), GRKs (Chen et al., 2001;Weiss et al., 2001) and now visual arrestins stands in striking contrast to the situation in rods, where typically only one isoform is expressed. A potentially valuable aspect of the expression of multiple isoforms of proteins in individual cells has been proposed in the context of the two great genome duplication events that are thought to have occurred early in vertebrate evolution (Sidow, 1996): multiple isoforms allow evolution to proceed more rapidly, as the primary function of the protein can be preserved by one variant, while mutations in the other allow novel or more restricted functions to evolve. It may be advantageous for cones, which are now understood to be the basal vertebrate photoreceptor type (Lamb et al., 2007;Reichenbach and Robinson, 1995), to retain multiple isoform expression, as this could allow vertebrates to radiate more readily into different photic environments. In contrast, the functioning of rods as single photon detectors may so tightly constrain transduction proteins to forms that minimize noise, that multiple isoforms are practically excluded.

Expression levels of Arr4 and Arr1 in cones

We estimated the quantity of Arr1 in cones to be ~ 50-fold higher than that of Arr4 (Table 1). The total quantity of visual arrestin stands in a 6:1 ratio to cone opsin, an approximately 7-fold higher ratio than Arr1 to rhodopsin in rods (Table 1; Supplement Table 1S). As is well established in rods (Elias et al., 2004;Philp et al., 1987;Strissel et al., 2006), in dark adapted cones the bulk of arrestin is found not in the outer, but rather in the inner segment (Fig. 3,Table

1). Again, in contrast to mouse rods, which in their dark adapted state have an Arr1 quantity in the outer segment of only a few percent of rhodopsin (Strissel et al., 2006), in cones the total quantity of visual arrestin in the outer segment is close to that of the cone opsin (Table 1).

A previous study reported an Arr4 expression level (0.006 pmol/retina) about 1% of that (~1 pmol/retina) estimated here, and based on this evidence concluded it unlikely that Arr4 could function in the shutoff of cone opsin (Chan et al., 2007). We can offer no certain explanation of this discrepancy, but suggest that the lower estimate could have arisen from relatively lower yields in dissection, combined with absence of control for the masking effect of retinal lysate on Arr4 immunoblot signals. Such masking, which can reach 20-fold or more, was controlled for in our experiments by addition of *Arr4*$^{-/-}$ lysate to recombinant Arr4 standards (cf. Supplement). The value 0.006 pmol/eye corresponds to only 1800 molecules of Arr4 in the cone outer segment, a concentration of 210 nM given a cone OS cytoplasmic volume of 14 μm^3 and that only 10% of the Arr4 is in the cone outer segment in the dark (Table 1) Since the highest second order rate for protein-protein interactions is ~ 10^6 M s^{-1} (Fersht, 1977), the predicted highest first order rate constant for Arr4 association with photoactivated cone opsin would be 210 × 10^{-9} M × 10^6 M^{-1} s^{-1} = 0.2 s^{-1}. Our physiological results indicate that Arr4 binds to cone opsin in *Arr1*$^{-/-}$ cones less than 0.1 s after photoactivation (see below), implying a rate constant exceeding 10 s^{-1}, 20-fold higher than that predicted, and thus that the actual concentration is substantially higher than 210 nM. In contrast, the concentration of Arr4 that we estimated for the dark adapted cone OS, 12 μM (Table 1), predicts an upper limit to Arr4 association with photoactivated cone opsin that readily accomodates the kinetics of the dim-flash response of *Arr1*$^{-/-}$ cones (Fig 8A).

Both Arr4 and Arr1 arrest photoactivated S- and M- cone opsins

By creating *Arr4*$^{-/-}$ mice (Fig. 1), and breeding *Arr4*$^{-/-}$ *Arr1*$^{-/-}$ double-knockout mice (*Arr*-DKO), and recording the light responses of S-dominant cones of each of the four genotypes – WT, *Arr4*$^{-/-}$, *Arr1*$^{-/-}$, *Arr*-DKO (Fig. 4 – Fig. 6) – we tested the hypothesis that one or both arrestins function to arrest native cone phototransduction. In the cones of *Arr*-DKO mice the inactivation of phototransduction following strong flashes is greatly slowed (Fig. 4J; Fig. 5), establishing an essential need for an arrestin for normal inactivation. The recoveries of responses of *Arr4*$^{-/-}$ and *Arr1*$^{-/-}$ cones revealed that expression of either arrestin is sufficient for nearly normal inactivation (Fig. 4D–F; G–I; Fig. 5). Finally, dim-flash responses of cones driven by either S-opsin or M-opsin (Fig. 6) exhibit the same requirement for an arrestin for fully normal recovery, establishing that *both* Arr1 and Arr4 function in arresting the activity of either cone opsin.

In light of the evidence presented here that Arr1 and Arr4 are both expressed in mouse cones, and that each is capable of arresting cone opsin function, results in two previous studies can be interpreted as consistent with our conclusions. Thus, the absence any slowing of the recovery of cone-driven ERGs in *Arr1*$^{-/-}$ mice (Lyubarsky et al., 2002), and likewise the absence of any difference between M-opsin dim-flash responses in WT and *Arr1*$^{-/-}$ mouse cones (Shi et al., 2007) can now be interpreted as due to the function of Arr4.

Much faster decay of photoactivated, phosphorylated cone- than rod- opsins

Only one photoreceptor-specific GRK, Grk1 (alias rhodopsin kinase, RK), is expressed in mouse photoreceptors (Caenepeel et al., 2004), and physiological evidence from rods of *Grk1*$^{-/-}$ mice has confirmed that phosphorylation by Grk1 is the necessary first step in normal inactivation of mouse rods (Chen et al., 1999a;Mendez et al., 2000). Grk1 has also been shown to phosphorylate photoactivated mouse cone opsins (Zhu et al., 2003), and Grk1 has been shown necessary for normal inactivation of mouse cones (Lyubarsky et al., 2000;Nikonov et al., 2005). Arr4 and Arr1 must play their role in arresting phosphorylated cone opsin activity

at least by the time when the dim-flash response of *Arr*-DKO cones peels off from the WT trace (Fig. 6, Fig. 8A). Thus, taking into consideration the 21 ms delay introduced by analog filtering, it can be concluded that in WT cones Arr4 or Arr1 binding to phosphorylated cone S- and M-opsins has occurred no later than 80 ms after a flash of light.

Differences between rods and cones without Arr1 in the dim-flash response

In the absence of both Arr1 and Arr4, the dim-flash response driven by photoactivated S- and M-opsin in cones recovers normally to within 45% of baseline, and then undergoes a slowed return to baseline with a time constant of 750 ms (Fig. 8A), ~ 2-fold faster than transgenic S-opsin recovery in *Arr1*$^{-/-}$ rods (Chan et al., 2007). In contrast, in the absence of Arr1, the rod dim-flash response shows a similar "slow tail" that decays to baseline with a time constant of 30 to 50 s (Chan et al., 2007;Shi et al., 2007;Xu et al., 1997). This greater than 50-fold difference between the decay of photoactivated rhodopsin and S-opsin in the absence of Arr1 has been attributed to the difference in Metarhodopsin II decay in rod- vs. cone opsins (Shi et al., 2007), though spectroscopic confirmation has not yet been presented.

The "slow-tail" phase of the recovery from saturating flashes reveals differences in the effectiveness of Arr1 and Arr4 in arresting S-opsin

Responses of WT, *Arr4*$^{-/-}$ and *Arr1*$^{-/-}$ cones recover from strongly saturating flashes in two distinct phases: a rapid initial phase which is approximately shape-invariant over change in intensity, followed by a "slow tail", whose amplitude increases with flash intensity (Fig. 4). Analysis of the slow tails reveals that they behave differently in cones of the three genotypes: thus, for a given flash intensity (say, 2×10^5 photons μm^{-2}), the slow tail has a higher amplitude in *Arr1*$^{-/-}$ cones than in *Arr4*$^{-/-}$ and WT cones (Fig. 8C–D). An hypothesis that might explain this result is that the Arr1 present in *Arr4*$^{-/-}$ cones is more effective in arresting the activity of an intermediate in the decay of S-opsin than is the lower quantity of Arr4 in *Arr1*$^{-/-}$ cones; the presumptive identity of the hypothesized intermediate is phosphorylated cone opsin, since Grk1 is expressed in all the genotypes investigated, and known to be essential to normal murine cone inactivation (see above). Integrating the data of all genotypes in Fig. 8 with a comprehensive hypothesis, however, will be challenging. A possibly related, interesting feature of *Arr*-DKO cones is that they exhibit a slow tail at *all* subsaturating intensities: thus, the slow tail that appears at the lowest intensities in *Arr*-DKO cones (Fig. 8A, red trace; 8C, red curve) is comparable in amplitude and kinetics to that seen in WT cones at ~ 70-fold higher intensities (Fig. 8C green curve).

Evolutionary perspective on the role(s) of Arr4 and Arr1 in cones

The phylogeny, binding partners and known functions of members of the four families of vertebrate arrestins have been summarized in a recent, thorough review (Gurevich & Gurevich, 2006). The ARR4 family, with members expressed in virtually all vertebrates, stands out in contrast to the other three families, in that until this report no function had been experimentally identified *in situ*, that is in the photoreceptor cells in which the protein is normally expressed. While our results showing Arr4 can arrest the activity of photoactivated cone opsins are consistent with the expectation derived from the thoroughly investigated role of ARR1 in quenching the activity of photoactivated rhodopsin, the evolutionary history and the distribution of Arr4 in cones suggests that additional roles for the protein remain to be discovered.

Cones are more closely related than rods to the phylogenetically basal ciliated photoreceptors from which both types of vertebrate photoreceptors derive (Reichenbach & Robinson, 1995; Lamb et al., 2007). Tunicates, which have a single arrestin gene (*Ci-Arr*), are now thought to be basal to the vertebrate line (Delsuc et al., 2006), yet split from the vertebrate lineage before the two main genome duplication events that likely gave rise to the other arrestin families

(Nordstrom et al., 2004;Sidow, 1996), Ci-Arr is expressed in the ciliated, hyperpolarizing photoreceptors of the larval tunicate, and is present throughout these cells, including their axons and synaptic specialization (Horie et al., 2005). It thus seems reasonable to hypothesize that additional Arr4 (and Arr1) binding partners and functions remain to be identified, particularly in the synaptic specialization of cones, where (as in tunicates) they reside in great abundance (Fig 3, Table 1).

METHODS

Nomenclature

The common nomenclature for members of the arrestin gene family expressed in mice is as follows (1) S-antigen (*Sag*); beta-adrenergic arrestins, *Arrb1* and *Arrb2*; cone-arrestin, or X-arrestin (*mCarr*), *Arr3*. As proposed by (Gurevich and Gurevich, 2006a), here we identify the four arrestin genes with a revised numerical nomenclature, so that *Sag* is *Arrestin1 (Arr1)* and *mCarr* is *Arrestin4* (*Arr4*).

Vertebrate animals

All procedures involving mice were approved by IACUCs of the University of Southern California and the University of Pennsylvania, and conformed to recommendations of the Association of Research for Vision and Ophthalmology. Due to their high susceptibility to light damage (Chen et al., 1999b), *Arr1*$^{-/-}$ mice were reared in constant darkness, and the same light-rearing conditions were adopted for *Arr4*$^{-/-}$ and arrestin double knockouts, while WT (*C57Bl6*) were maintained in cyclic illumination. For all biochemical, histological or physiological experiments mice were dark adapted for at least 24 hrs. Euthanasia was performed under dim red light, and all subsequent manipulations under infrared illumination.

Creation and characterization of Arr4$^{-/-}$ knockout mice

The organization of the *Arr4* gene, the gene targeting strategy for creating *Arr4*$^{-/-}$ mice, and confirmation of null expression of Arr4 is presented in the context of Fig. 1. Further details are presented in the Supplement.

Quantitative immunoblotting of Arr4

A full length cDNA for *Arr4* was obtained from a mouse retinal cDNA library (Pierce et al., 1999), modified to encode a 5′ hexahistidine tag, ligated into the pFastBac1 (Invitrogen) plasmid, and transformed into One Shot Top10 (Invitrogen) *E. coli*. Sequence-verified plasmids were transformed into DH10Bac *E. coli*. High titer baculovirus was added to Sf9 cells in suspension culture to produce recombinant Arr4 (rArr4); the latter was extracted and purified, and its concentration determined spectrophotometrically. Aliquots of retinal lysates quantified with rhodopsin bleaching difference spectroscopy were subjected to SDS-PAGE and the Arr4 content determined by comparison of their immunoblot signals with those of known quantities of rArr. (see Supplement for details)

Confocal microscopy and quantitation of immunohistochemistry

Eyes were enucleated under infrared illumination after lid removal and careful severing of the extraocular muscles with a scalpel to minimize distortion of retinal tissue. After a slit was made in the cornea, the enucleated eye was fixed in 4% paraformaldehyde for 30 min, and then the cornea and lens removed and fixation continued in 4% formaldehyde at 4°C for no more than 24 hr; the eyecups were put in 30% sucrose overnight at 4°C and then embedded in OCT. Cryosections were exposed to blocking buffer (1% BSA, 1% NGS, 1% Triton X-100 in 1X PBS) for 30 min, and then to anti-Arr1 (D9F2, mouse monoclonal) or anti-Arr4 (LUMIj, rabbit polyclonal) primary antibodies, and to appropriate secondaries. When both D9F2 and LUMIj

were employed, the 7-step protocol used was as follows: (1) LUMIj (dilution 1:500) 2h at room temperature (RT), (2) 3× 10 min washes with PBS; (3) Alexa555-conjugated goat anti-rabbit (1:200) 1h at RT; (4) 3× 10 min washes; (4) D9F2 (1:20,000) overnight at 4C; (5) 3× 10 min washes; (6) Alexa488-conjugated donkey anti-mouse (1:200) 1h at RT; (7) 3× 10 min washes with PBS.

Confocal imaging was performed with a Zeiss LSM-510 microscope using a 63X oil immersion lens, and appropriate dichroic beamsplitters. Only sections exhibiting integrity of the outer segment layer and the photoreceptor/RPE interface, as confirmed with differential interference contrast (DIC), were scanned. Confocal z-stacks were collected in a sampling scheme that interlaced DIC, Alexa488 and Alexa555 fluorescence, with resolution 0.1 μm in the *x*-, *y*-dimensions, and 0.3 μm in *z*. Laser intensities and photomultiplier settings were set so that the z-stack had negligible saturated voxels. Image data were analyzed with customized MatLab™ (Mathworks, Natick, MA) software modified from that previously described (Peet et al., 2004); this software enabled the user to "cookie cut" individual cone cells visualized by the anti-Arr4 antibody LUMIj out of the 3D z-stack, and analyze the distribution of fluorescence in the cone's various compartments.

Electrophysiology

Mouse cone photoresponses from ventral retina were recorded with suction electrodes using the methods of (Nikonov et al., 2006). Special care was taken to monitor the stability of the responses of individual cones over a recording session, which often lasted an hour or more and involved the collection of up to 2000 light responses (Supplement). Light responses to dim and strong flashes obtained at the beginning and end of the period from which responses were collected from a cone were compared, and only cells for which the two sets of responses remained unchanged were included in the report. The genotype of each mouse from whose retina recordings were made was confirmed with PCR analysis (Supplement). Statistical analysis of response properties included 1-way ANOVAs, with genotype as the treatment and the various measured parameters of the cones as the dependent variable (Table 2), and linear and quadratic regression trend analysis, as described in Hays (963) (Fig. 5).

Supplementary Material

Refer to Web version on PubMed Central for supplementary material.

References

Caenepeel S, Charydczak G, Sudarsanam S, Hunter T, Manning G. The mouse kinome: discovery and comparative genomics of all mouse protein kinases. Proc. Natl. Acad. Sci. U. S A 2004;101:11707–11712. [PubMed: 15289607]

Carter-Dawson LD, LaVail MM. Rods and cones in the mouse retina. I. Structural analysis using light and electron microscopy. J. Comp Neurol 1979;188:245–262. [PubMed: 500858]

Chan S, Rubin WW, Mendez A, Liu X, Song X, Hanson SM, Craft CM, Gurevich VV, Burns ME, Chen J. Functional comparisons of visual arrestins in rod photoreceptors of transgenic mice. Invest Ophthalmol Vis. Sci 2007;48:1968–1975. [PubMed: 17460248]

Chen CK, Burns ME, Spencer M, Niemi GA, Chen J, Hurley JB, Baylor DA, Simon MI. Abnormal photoresponses and light-induced apoptosis in rods lacking rhodopsin kinase. Proc. Natl. Acad. Sci. U. S. A 1999a;96:3718–3722. [PubMed: 10097103]

Chen CK, Zhang K, Church-Kopish J, Huang W, Zhang H, Chen YJ, Frederick JM, Baehr W. Characterization of human GRK7 as a potential cone opsin kinase. Mol. Vis 2001;7:305–313. [PubMed: 11754336]

Chen J, Simon MI, Matthes MT, Yasumura D, LaVail MM. Increased susceptibility to light damage in an arrestin knockout mouse model of Oguchi disease (stationary night blindness) CHEN1999. Invest Ophthalmol Vis. Sci 1999b;40:2978–2982. [PubMed: 10549660]

Craft CM, Whitmore DH, Wiechmann AF. Cone arrestin identified by targeting expression of a functional family. Journal of Biological Chemistry 1994;269(6):4613–4619. [PubMed: 8308033]

Delsuc F, Brinkmann H, Chourrout D, Philippe H. Tunicates and not cephalochordates are the closest living relatives of vertebrates. Nature 2006;439:965–968. [PubMed: 16495997]

Elias RV, Sezate SS, Cao W, McGinnis JF. Temporal kinetics of the light/dark translocation and compartmentation of arrestin and alpha-transducin in mouse photoreceptor cells. Mol. Vis 2004;10:672–681. [PubMed: 15467522]

Fersht, A. Enzyme Structure and Mechanism. San Francisco: W. H. Freeman; 1977.

Gurevich EV, Gurevich VV. Arrestins: ubiquitous regulators of cellular signaling pathways. Genome Biol 2006a;7:236. [PubMed: 17020596]

Gurevich VV, Gurevich EV. The structural basis of arrestin-mediated regulation of G-protein-coupled receptors. Pharmacol. Ther 2006b;110:465–502. [PubMed: 16460808]

Hays, WL. Statistics for psychologists. New York: Holt, Rinehart and Winston; 1963.

Horie T, Orii H, Nakagawa M. Structure of ocellus photoreceptors in the ascidian Ciona intestinalis larva as revealed by an anti-arrestin antibody. J. Neurobiol 2005;65:241–250. [PubMed: 16118796]

Jeon CJ, Strettoi E, Masland RH. The major cell populations of the mouse retina. J. Neurosci 1998;18:8936–8946. [PubMed: 9786999]

Kuhn H, Hall SW, Wilden U. Light-induced binding of 48-kDa protein to photoreceptor membranes is highly enhanced by phosphorylation of rhodopsin. FEBS Lett 1984;176:473–478. [PubMed: 6436059]

Lamb TD, Collin SP, Pugh EN Jr. Evolution of the vertebrate eye: opsins, photoreceptors, retina and eye cup. Nat. Rev. Neurosci 2007;8:960–976. [PubMed: 18026166]

Lyubarsky AL, Chen C, Simon MI, Pugh EN Jr. Mice lacking G-protein receptor kinase 1 have profoundly slowed recovery of cone-driven retinal responses. J. Neurosci 2000;20:2209–2217. [PubMed: 10704496]

Lyubarsky AL, Daniele LL, Pugh EN Jr. From candelas to photoisomerizations in the mouse eye by rhodopsin bleaching in situ and the light-rearing dependence of the major components of the mouse ERG. Vision Res 2004;44:3235–3251. [PubMed: 15535992]

Mendez A, Burns ME, Roca A, Lem J, Wu LW, Simon MI, Baylor DA, Chen J. Rapid and reproducible deactivation of rhodopsin requires multiple phosphorylation sites. Neuron 2000;28:153–164. [PubMed: 11086991]

Nikonov SS, Daniele LL, Zhu XM, Craft CM, Swaroop A, Pugh EN. Photoreceptors of Nrl(−/−) mice coexpress functional S- and M-cone opsins having distinct inactivation mechanisms. Journal of General Physiology 2005;125:287–304. [PubMed: 15738050]

Nikonov SS, Kholodenko R, Lem J, Pugh EN. Physiological features of the S-and M-cone photoreceptors of wild-type mice from single-cell recordings. Journal of General Physiology 2006;127:359–374. [PubMed: 16567464]

Nordstrom K, Larsson TA, Larhammar D. Extensive duplications of hototransduction genes in early vertebrate evolution correlate with block (chromosome) duplications. Genomics 2004;83:852–872. [PubMed: 15081115]

Peet JA, Bragin A, Calvert PD, Nikonov SS, Mani S, Zhao X, Besharse JC, Pierce EA, Knox BE, Pugh EN Jr. Quantification of the cytoplasmic spaces of living cells with EGFP reveals arrestin-EGFP to be in disequilibrium in dark adapted rod photoreceptors. J. Cell Sci 2004;117:3049–3059. [PubMed: 15197244]

Pepperberg DR, Cornwall MC, Kahlert M, Hofmann KP, Jin J, Jones GJ, Ripps H. Light-dependent delay in the falling phase of the retinal rod photoresponse. Vis.Neurosci 1992;8:9–18. [PubMed: 1739680]

Philp NJ, Chang W, Long K. Light-stimulated protein movement in rod photoreceptor cells of the rat retina. FEBS Lett 1987;225:127–132. [PubMed: 2826235]

Pierce EA, Quinn T, Meehan T, McGee TL, Berson EL, Dryja TP. Mutations in a gene encoding a new oxygen-regulated photoreceptor protein cause dominant retinitis pigmentosa. Nat. Genet 1999;22:248–254. [PubMed: 10391211]

Pugh EN Jr, Lamb TD. Amplification and kinetics of the activation steps in phototransduction. Biochim. Biophys. Acta 1993;1141:111–149. [PubMed: 8382952]

Reichenbach A, Robinson SR. Phylogenetic constraints on retinal organization and development. Progress in Retinal and Eye Research 1995;15:139–171.

Shi G, Yau KW, Chen J, Kefalov VJ. Signaling properties of a short-wave cone visual pigment and its role in phototransduction. J. Neurosci 2007;27:10084–10093. [PubMed: 17881515]

Sidow A. Gen(om)e duplications in the evolution of early vertebrates. Curr. Opin. Genet. Dev 1996;6:715–722. [PubMed: 8994842]

Strissel KJ, Sokolov M, Trieu LH, Arshavsky VY. Arrestin translocation is induced at a critical threshold of visual signaling and is superstoichiometric to bleached rhodopsin. J. Neurosci 2006;26:1146–1153. [PubMed: 16436601]

Weiss ER, Ducceschi MH, Horner TJ, Li A, Craft CM, Osawa S. Species-specific differences in expression of G-protein-coupled receptor kinase (GRK) 7 and GRK1 in mammalian cone photoreceptor cells: implications for cone cell phototransduction. J. Neurosci 2001;21:9175–9184. [PubMed: 11717351]

Wilden U, Hall SW, Kuhn H. Phosphodiesterase activation by photoexcited rhodopsin is quenched when rhodopsin is phosphorylated and binds the intrinsic 48-kDa protein of rod outer segments. Proc. Natl. Acad. Sci. U. S A 1986;83:1174–1178. [PubMed: 3006038]

Xu J, Dodd RL, Makino CL, Simon MI, Baylor DA, Chen J. Prolonged photoresponses in transgenic mouse rods lacking arrestin. Nature 1997;389(6650):505–509. [PubMed: 9333241]

Zhu X, Brown B, Li A, Mears AJ, Swaroop A, Craft CM. GRK1-dependent phosphorylation of S and M opsins and their binding to cone arrestin during cone phototransduction in the mouse retina. J. Neurosci 2003;23:6152–6160. [PubMed: 12853434]

Zhu X, Li A, Brown B, Weiss ER, Osawa S, Craft CM. Mouse cone arrestin expression pattern: light induced translocation in cone photoreceptors. Mol. Vis 2002;8:462–471. [PubMed: 12486395]

Zhu X, Wu K, Rife L, Brown B, Craft CM. Rod Arrestin Expression and Function in Cone Photoreceptors. Invest. Ophthalmol. Vis. Sci 2005;46:1179.

Acknowledgements

The authors acknowledge Drs. Xuemei Zhu, Marie Burns, Lauren Daniele, Jon Peet, Jasmine Zhao and Kebin Wu for their scientific contributions to this work, and thank Dr. Jeannie Chen for *Arr1*$^{-/-}$ mice. CMC is the Mary D. Allen Chair in Vision Research, Doheny Eye Institute (DEI) and Research to Prevent Blindness Senior Scientist. ENPJr is Jules and Doris Stein Research to Prevent Blindness Professor. Support: EY01581, GM79910 (CMC); EY02660, EY016453 (ENP), RPB Foundation (CMC, ENP); Fred & Dorie Miller and the William Hansen Sandberg Memorial Foundation (CMC), and the Paul & Evanina Bell Mackall Foundation Trust (ENP).

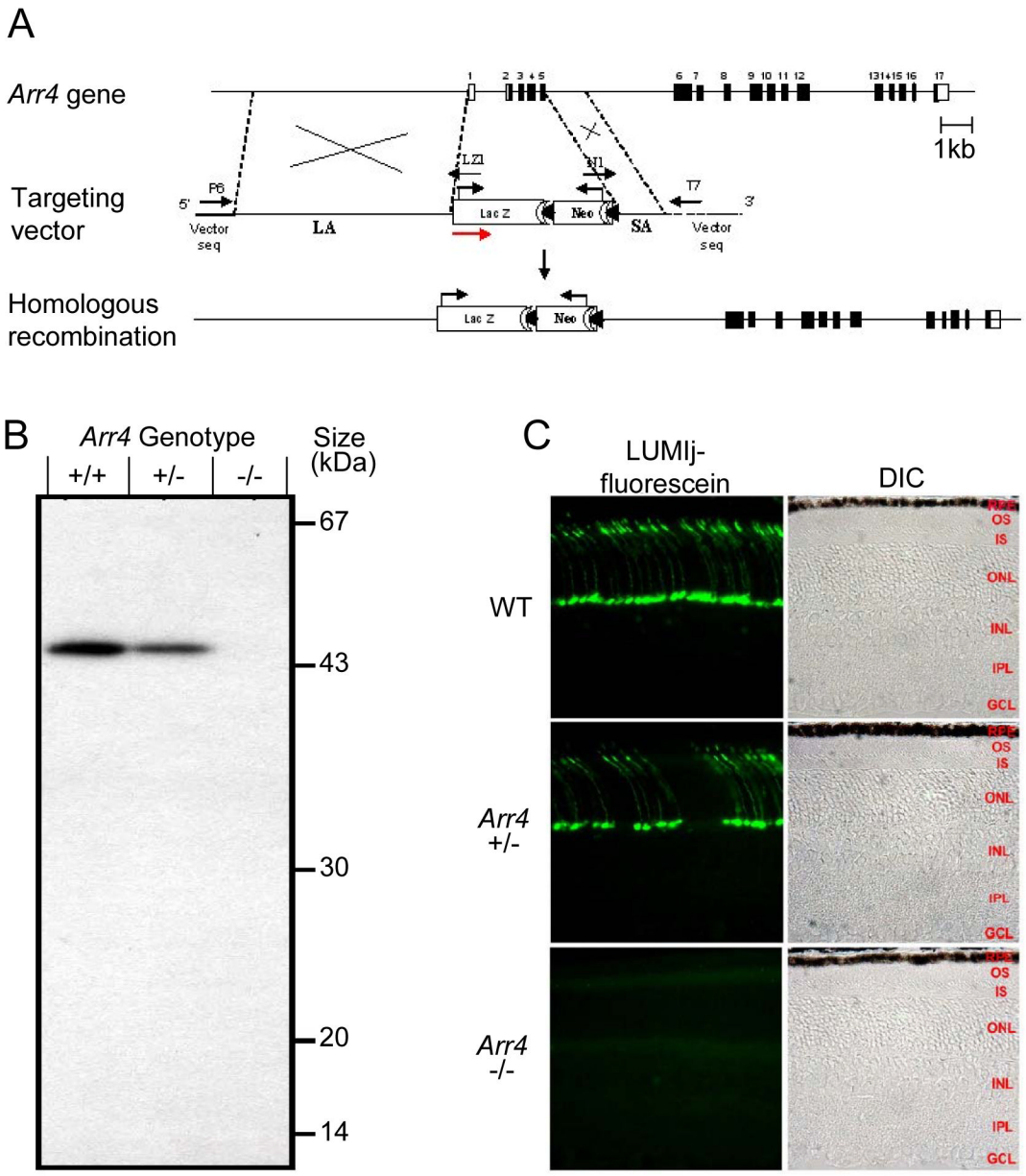

Figure 1. Strategy for creating and confirming Arrestin 4 knockout mice

A. **Organization of the mouse cone arrestin** (*mCarr, Arr4*) **gene** (Zhu et al., 2002b), the targeting construct and the recombinant allele. The genomic fragment from the 5'-noncoding region in exon 1 to exon 5 was replaced by the *LacZ/Neo* cassette. The translation start sites of the *LacZ* and *Neo* genes are identified by black arrows. The red arrow indicates the 5' → 3'direction of the construct. LA, long arm, SA, short arm. LZ1, N1, P6 and T7 are primer designations used for PCR genotyping amplification and sequencing the final construct.

B. **Immunoblot confirmation of knockout**. 50 micrograms of protein from total retinal homogenates from each genotype was resolved on an 11.5% SDS-PAGE, transferred to a PVDF membrane, and analyzed with ECL detection kit after incubation with the anti-Arr4 polyclonal antibody LUMIj and the appropriate secondary goat-anti-rabbit HRP-conjugated

antibody. A 45 kDa immunoreactive band was obtained in WT and in the heterozygote, while no immunoreactivity for mice with the targeted locus (*Arr4*$^{-/-}$) was seen.

C. **Immunohistochemical confirmation**. Frozen eyes were prepared and sectioned at 7 μm thickness through the optic nerve and stained with Arr4-LUMIj and a fluorescein-conjugated anti-rabbit secondary antibody. No immunoreactivity was detected in mice with the targeted locus. Abbreviations on the phase contrast images: RPE, retinal pigment epithelium; OS, outer segment layer, IS; inner segment layer; ONL, outer nuclear layer; INL, inner nuclear layer; IPL, inner plexiform layer; GCL, ganglion cell layer.

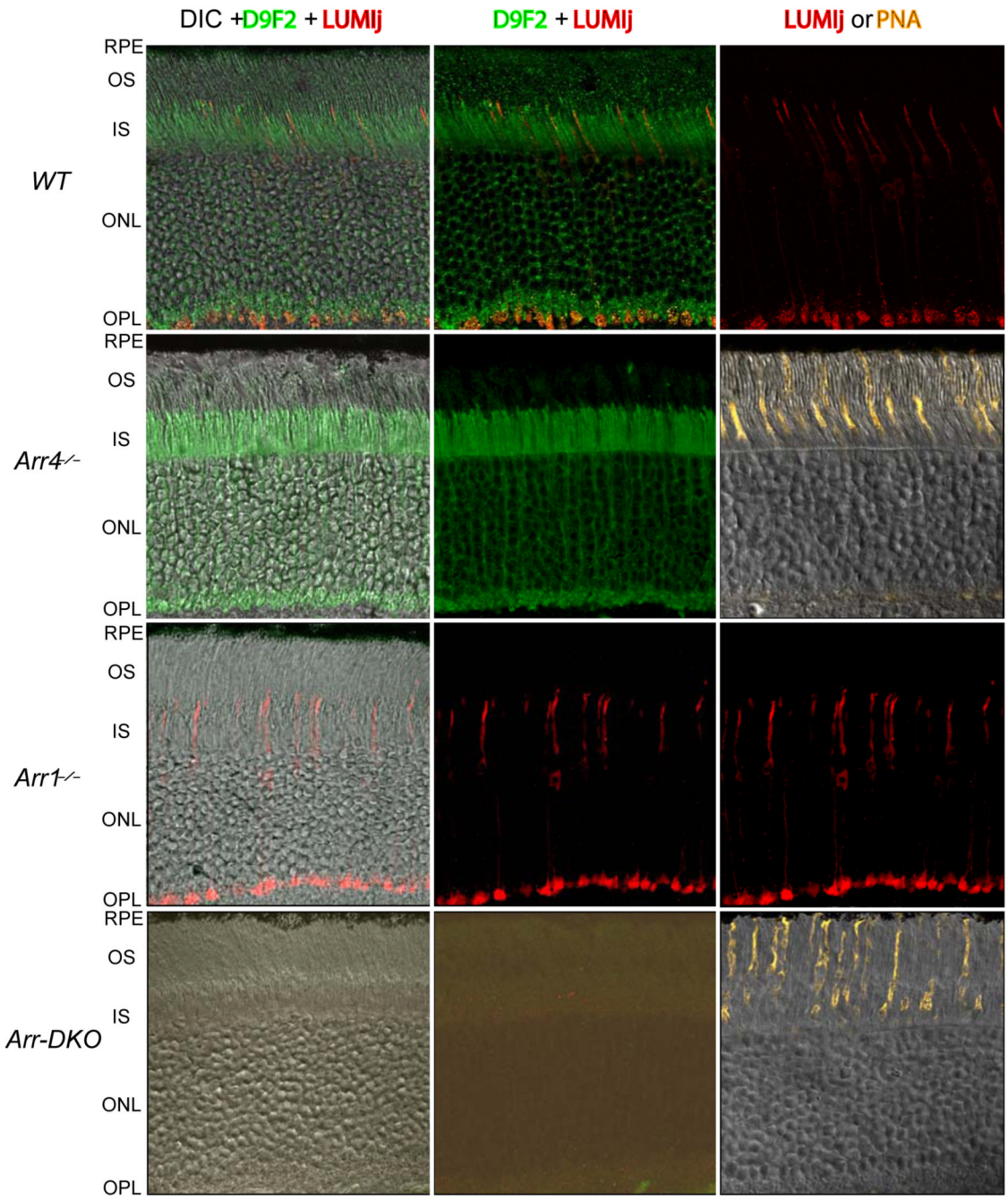

Figure 2. Distributions of Arr1 and Arr4 in the dark adapted retina

Each row of panels depicts confocal images of cryosections of a single retina of a mouse of the genotype specified at the left of the row. Images in the first column combine differential interference contrast (DIC), immunostaining with a secondary antibody (Ab) (red channel) against the anti-Arr4 primary Ab LUMIj, and with a secondary (green channel) against the anti-Arr1 primary D9F2. Images in the second column are identical to those in the first column, except for elimination of the DIC display. In all cases the cryosections were exposed to both Arr4- and Arr1- primaries and secondaries with exactly the same incubation procedure, and imaged with exactly the same settings of the confocal microscope. Thus, the absence of fluorescence in the red channel in the case of the cryosections of the *Arr4*$^{-/-}$ and *Arr*-DKO

retinas reflects an absence of D9F2-immunogenicity. Images in the third column are positive controls for the presence of cones: in genotypes in which Arr4 is expressed, the images simply show the LUMIj immunogenicity alone; for the two genotypes in which Arr4 is absent, a confocal fluorescence image of a section from the same retina stained with Alexa555 conjugated to PNA, which binds specifically to the cone sheath, is displayed. (Mouse cone outer segments (COS) are ~ 13 μm in length (Carter-Dawson & LaVail, 1979), and thus terminate about 10 μm short of the RPE; the PNA-stained sheath, which attaches to the RPE, bridges the gap.) The image in the middle column of the *Arr*-DKO row has been "stretched" so that the lowermost 10% of the intensity range is displayed, revealing negligible non-specific fluorescence. (See Supplement for additional details.)

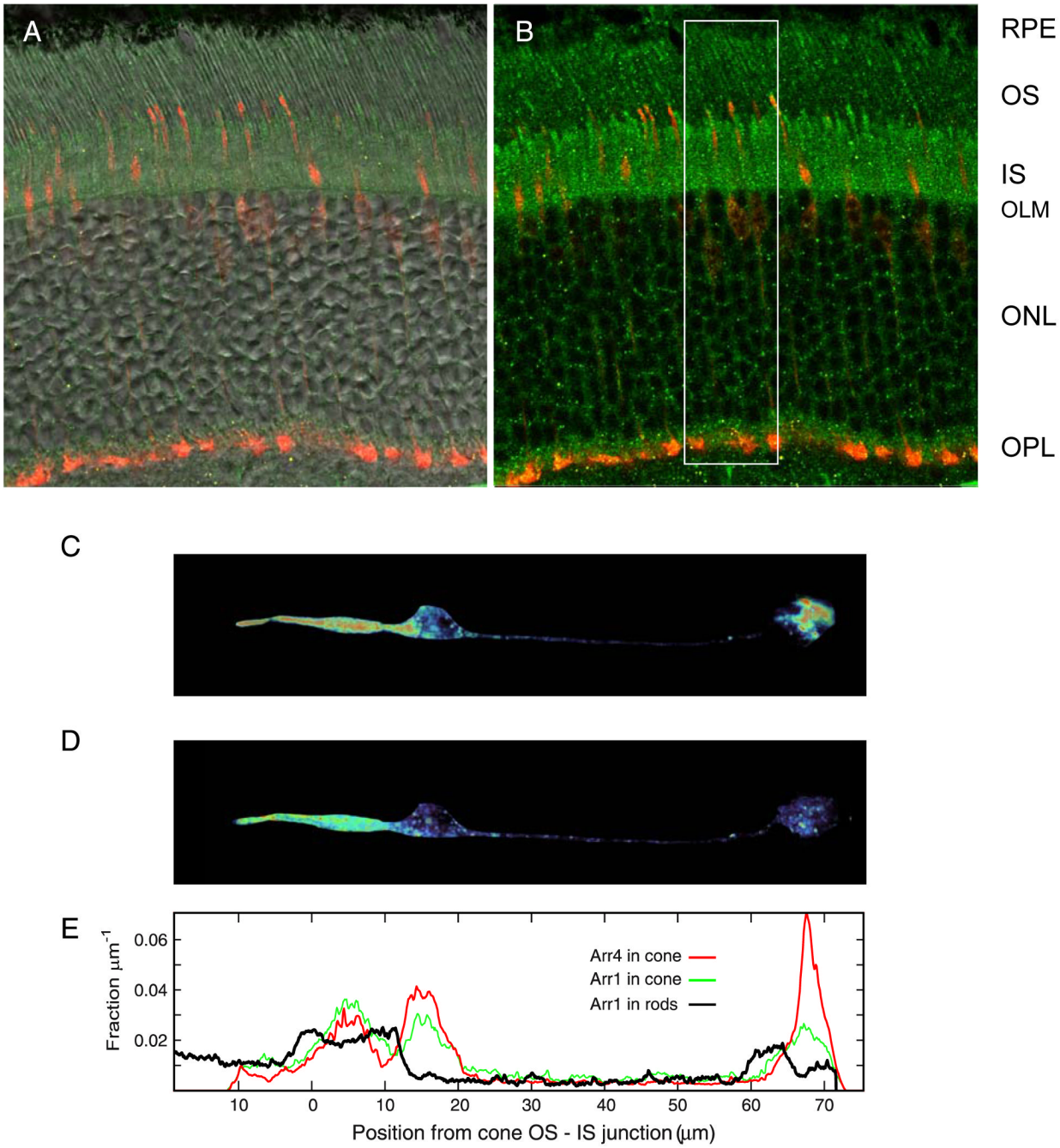

Figure 3. Distributions of Arr1 & Arr4 in dark adapted WT mouse cones

A. Confocal image of WT mouse retina crysection, overlaying immunofluorescence of Arr1-Ab (D9F2, green channel), Arr4-Ab (LUMIj, red channel) superimposed on differential interference contrast (DIC) image. (Abbreviated labels for retinal layers as in Fig. 1; OLM = outer limiting membrane) B. Same image as in A, with DIC removed. C. Pseudo-color display of the Arr4-Ab fluorescence of one of the cones of the cryosection of A, which has been "cookie cut" from the 3D z-stack matrix and projected onto a single plane (red represents most intense fluorescence, dark blue absence of fluorescence). Arr4 is seen to be most concentrated in the IS region, the outermost portion of the cell body and in the synaptic pedicle. D. Pseudocolor image of Arr1 immunogenicity, obtained from the immunofluorescence in the "green" (D9F2-

Alexa488) channel of the voxels corresponding to the cone as "cut" on the "red" (LUMIj-Alexa555) channel. E. Distribution of Arr4 (red trace) and Arr1 (green trace) immunogenicity in the cone of panels C, D along the radial axis of the retina (the *x*-axis in E corresponds precisely to those in C, D). The black trace shows the radial distribution of Arr1 in the slab defined by the white bounding box in panel B, and extending 0.9 μm in either direction in the confocal z-stack; this trace was obtained by integrating the D9F2-specific immunofluorescence across the *y*- and *z*-dimensions of the bounding volume. Note that the trace (red) for Arr4 extends 11 μm to the left from the OS-IS junction; the length of this COS is close to that (13.4 ± 0.7 μm) of a population of mouse COS studied by Carter-Dawson & LaVail (1979). (A number of critical issues and assumptions – such as the absence of material epitope masking – are involved in using immunofluorescence to quantify the distribution of Arr1 and Arr4; these are addressed in detail in the Supplement.)

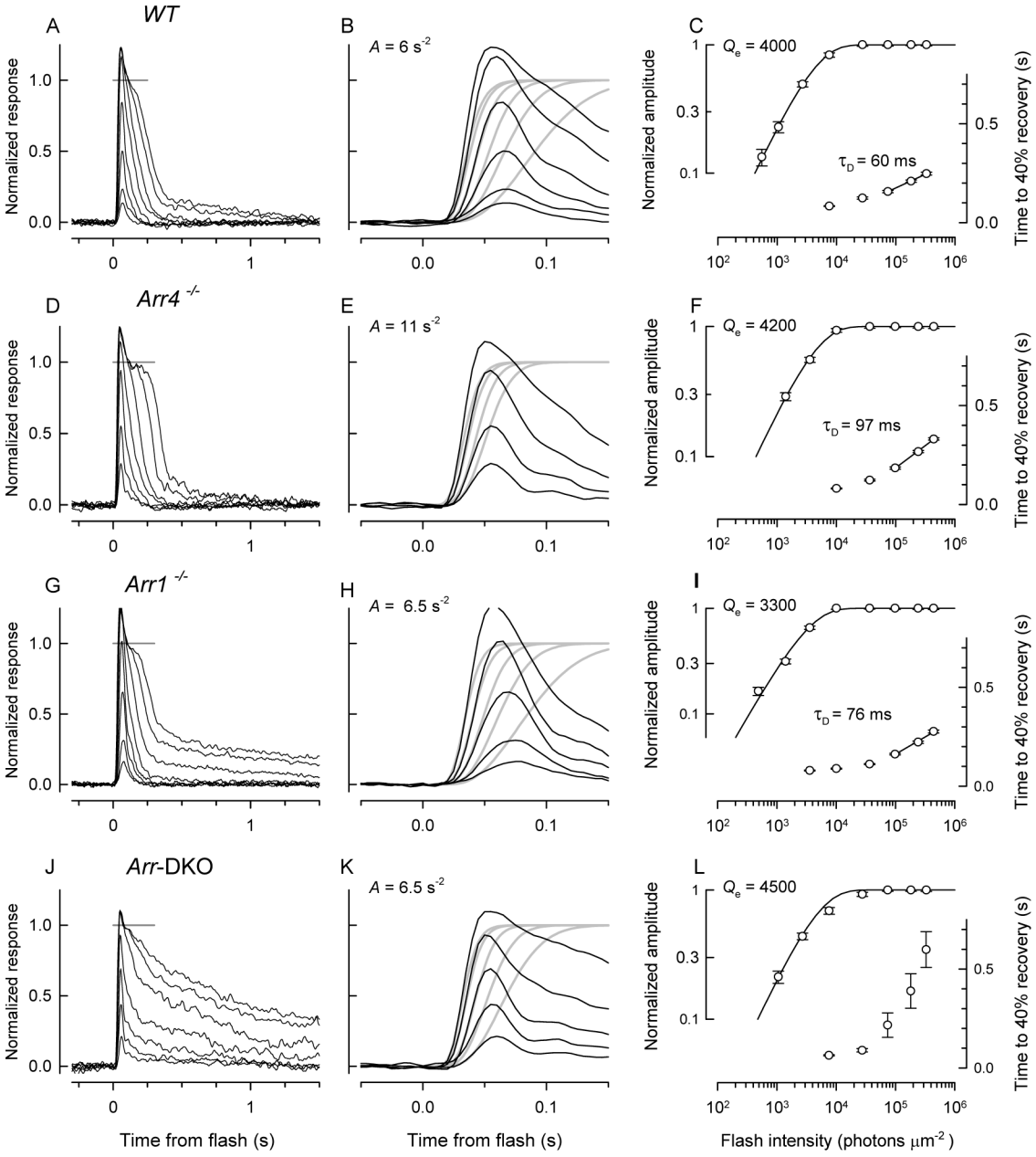

Figure 4. Light response families & kinetic analyses of S-dominant mouse cones

Each row of panels illustrates a family of responses to 361 nm flashes and attendant analyses for an S-dominant cone of a mouse of one of the four genotypes: WT (A – C), *Arr4*$^{-/-}$ (D – F), *Arr1*$^{-/-}$ (G – I) and *Arr4*$^{-/-}$ *Arr1*$^{-/-}$ double-knockout (DKO; J – L). The traces in the light response families (A, D, G, J) represent the average of 60 – 100 responses to the dimmest flashes and 20 – 30 responses to the most intense flashes; the gray line near the top of each panel is an estimate of the level of the light-sensitive current (the current above the line is not light-sensitive, and is presumed to be a voltage-activated current). The middle column of panels (B, E, H, K) replot traces to the lower intensity light flashes at left on an expanded time base, where they are fitted with theoretical traces (gray) to extract the amplification constant, *A*, of phototransduction given on the plot (cf. Methods). For this analysis, the traces have been normalized by the light sensitive current (dashed gray line in panels A, D, G, J). The rightmost

panels (C, F, I, L) plot as a function of flash intensity the response amplitudes of the family at left and the time to 40% recovery (T_{40}) from the saturating flashes. The amplitude vs. intensity data have been fitted with an exponential saturation function to extract the intensity level (Q_e) that reduces the amplitude to 1/e and the recovery data were fitted with a straight line on the semilog plot to estimate the "Pepperberg" or dominant recovery time constant (τ_D). The normalization of the traces for amplification analysis excludes the "nose": the rationalization for this is provided in the Supplement, Fig. 10S, where it is shown that the plateau level following the "nose" is the zero level of the light-sensitive current. The amplification analysis was not applied to the saturating responses that exhibit "noses".

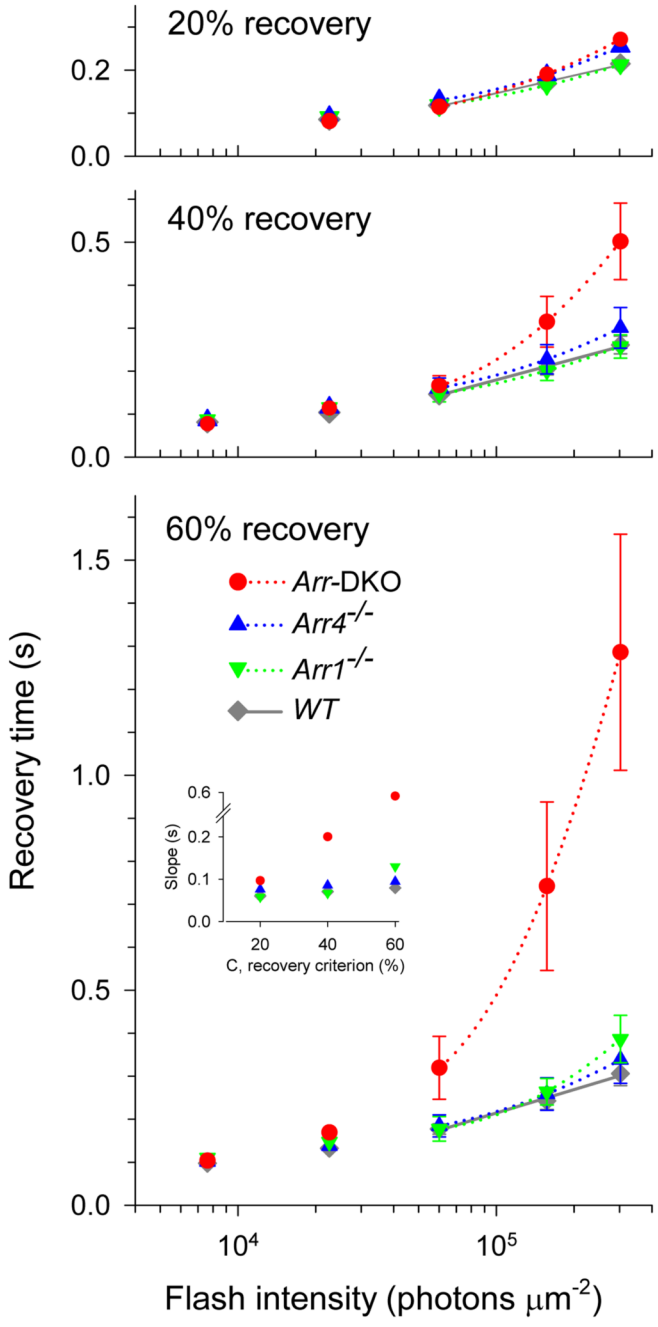

Figure 5. Recovery times of S-dominant cones of WT, Arr4$^{-/-}$, Arr1$^{-/-}$ and Arr-*DKO* mice

The three panels are each Pepperberg plots, i.e., show as a function of the logarithm of the flash intensity the time T_C for cones of each genotype to recover criterion levels (C) of 20%, 40% or 60% respectively of their light sensitive current after saturating flashes (c*f*. Fig. 4). The values at a set of discrete intensities were interpolated from individual cone's records, and then averaged over genotype; the error bars are ± 2 s.e.m. Linear and quadratic regression functions were fitted by least squares to the "T_C vs log I" data for saturating flashes only (the quadratic regression functions are illustrated): in no case did the addition of the quadratic term contribute significantly to reducing the variance about the regression line, and thus in each case a linear regression function suffices. [The least squares analysis was done with the Matlab™ "regress"

script: the statistical test for nonlinear LS regression is described in Hays, 1963, p. 545, and yielded an $F(df_1,df_2)$-statistic with df_1=1 and df_2 = 75 (WT), 29 (*Arr4*$^{-/-}$), 24 (*Arr1*$^{-/-}$), 48 (*Arr*-DKO), and in no case was $F > 1$, i.e. all instances highly insignificant.] For *WT*, *Arr4*$^{-/-}$ and *Arr1*$^{-/-}$ cones the slopes of the "T_C vs log I" data are *roughly* constant across level C and genotype, in contrast, with the *Arr*-DKO data, for which the slope change strongly with C. These points are illustrated in the *inset* in the lowermost panel which plots the *Slopes* vs. C for each genotype. Though much less than for the *Arr*-DKO data, for *WT*, *Arr4*$^{-/-}$ and *Arr1*$^{-/-}$ there are orderly increases in slope with C; e.g., for the WT data the slopes are 60 ms (C = 20% recovery), 70 ms (C = 40 %) and 79 ms (C = 60%). In Table 2 we have taken the slope for the criterion C = 40% as the estimate of τ_D, the dominant recovery time constant (Pepperberg constant).

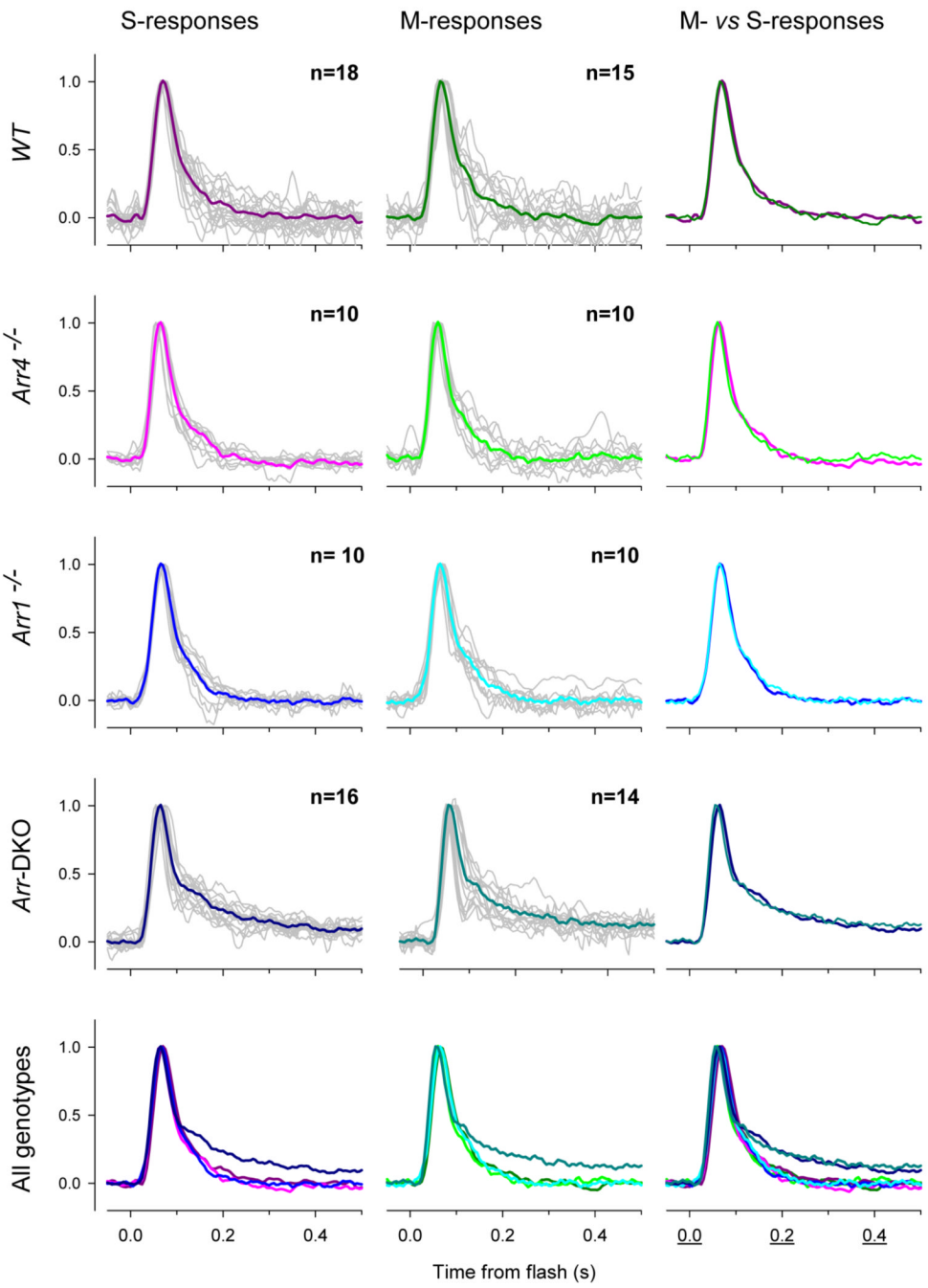

Figure 6. S- and M-opsin driven dim flash responses of cones lacking one or both visual arrestins

The first column of panels illustrates the dim-flash responses of cones of mice of the genotypes indicated at left and stimulated with 361 nm flashes that photoactivate only S-opsin; the responses of individual cones are shown as gray traces, while the colored traces show the averaged trace. The second column of panels shows the responses of the same cones stimulated with 510 nm flashes that activate only the M-opsin that is co-expressed in the same cones (Nikonov *et al.*, 2006). The third column compares the averaged S-opsin and M-opsin driven responses. The final row of the figure compares the averaged responses of cone of the four different genotypes, with the colors repeated from the average traces presented above.

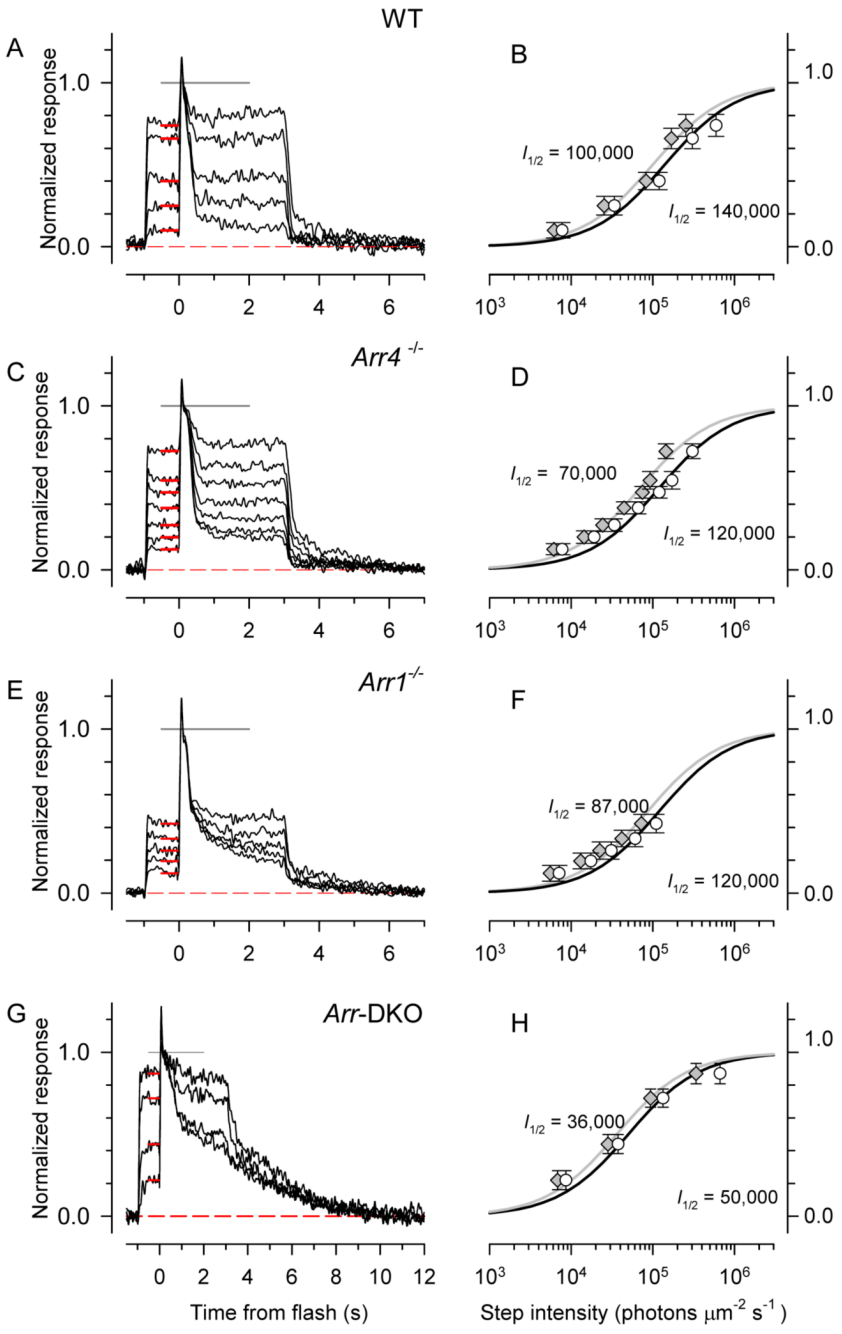

Figure 7. Step response families of S-dominant cones

Panels A, C, E, G show step response families for S-dominant cones of mice of the different genotypes investigated. Steps of light of 361 nm light of increasing intensity were applied at $t = -1$; at $t = 0$ a saturating flash was delivered to determine the maximum level of the light-sensitive current (estimated as the gray line at amplitude 1.0). The red bars plot the average level of the response to the light steps, which are replotted in the right-hand panel of each row as a function of step intensity (open circles), and fitted with a hyperbolic saturation function to extract the half-saturating intensity ($I_{½}$). The gray symbols replot the white symbols, but the intensities have been corrected for the estimated level of S-opsin bleaching (Nikonov *et al.*, 2006).

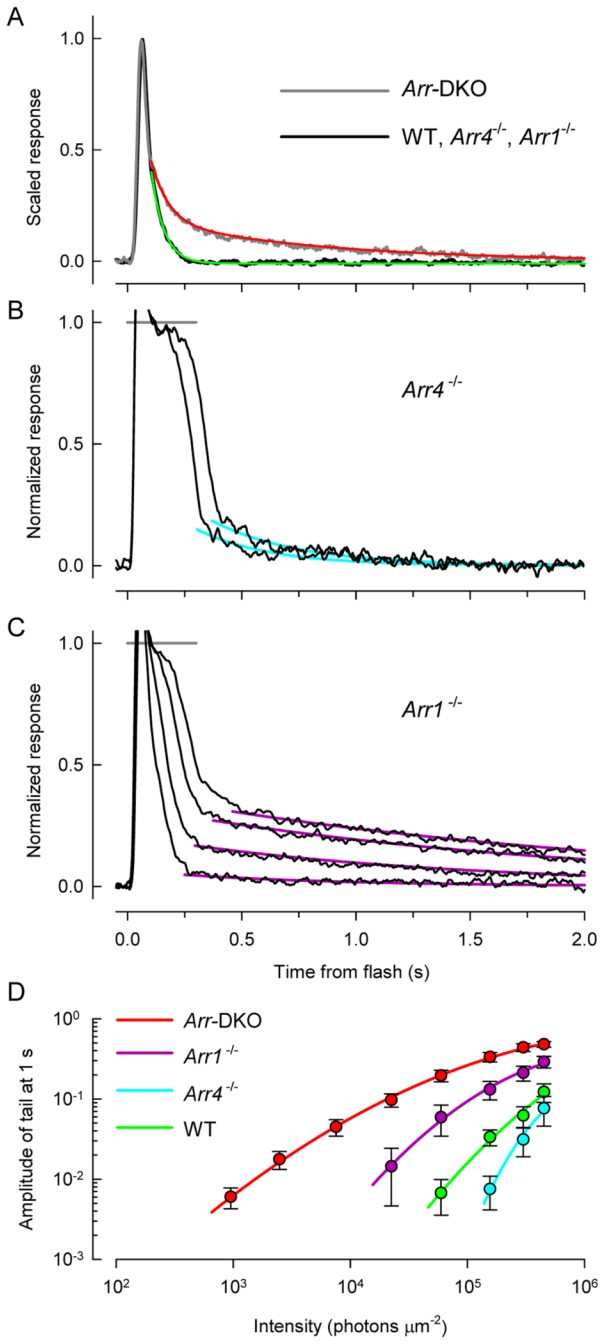

Figure 8. Response tail phases depend on arrestin genotype

A. *Dim flash responses*. The noisy black trace presents the grand average dim-flash responses of cones that express only Arr4 ($Arr1^{-/-}$), only Arr1 ($Arr4^{-/-}$) or both arrestins (WT); the noisy gray trace is the averaged dim-flash response of *Arr*-DKO cones (cf Fig. 5, last row of traces). Both averages combine S- and M-opsin driven responses, which had indistinguishable forms in each genotype. The smooth green trace is an exponential decay, $r(t) = r(t_0)\exp[-(t - t_0)/\tau)]$, with $t_0 = 0.1$ s, $\tau = 55$ ms, and $r(t_0) = 0.45$, while the red trace is a decaying double exponential of the form

$$r(t)=r(t_0)\{a_1\exp[-(t-t_0)/\tau_1)]+a_2\exp[-(t-t_0)/\tau_2)]\},$$

with t_0 and $r(t_0)$ as before, and a_1= 0.27, a_2= 0.18, τ_1 = 73 ms, and τ_2 = 750 ms.
B–C. *Responses to saturating flashes* of *Arr4*$^{-/-}$ cone (from Fig. 4D) and of *Arr1*$^{-/-}$ cone (from Fig. 4G). The tail phases of the responses have been fitted with first-order exponential decays.
D. Summary analysis of the tail phase responses of all the cones investigated (see Table 2 for n's). The tail phase of each saturating response of every cone was fitted with exponential decays as in panel B, C, and the amplitude of the tail estimated from the fitted curve at t = 1.0 s after the flash; the values at a set of discrete intensities were interpolated, and averaged over genotype. The error bars are ± 2 s.e.m.

Table 1

Estimated quantities of Arr1 and Arr4 in subcellular compartments of WT cones

Quantity (unit)	Whole Cone	Outer segment	Inner segment	Cell body	Axon	Pedicle
Volume (μm^3; fraction)	**950 ± 220**	**0.05**[b]	**0.14**	**0.30**	**0.20**[b]	**0.30**
Arr4 (molecules; fractions)	**3.3×10^6**	**0.10**	**0.16**	**0.22**	**0.10**	**0.42**
Arr1 (molecules; fractions)	**1.7×10^8**	**0.11**	**0.22**	**0.18**	**0.19**	**0.30**
Arr4 (concentration, μM)		**12**	**6.6**	**4.2**	**2.9**	**8.1**
Arr1 (concentration, μM)		**650**	**470**	**180**	**280**	**300**

The topmost row identifies the regions of the cone characterized, while entries in the centermost column identify the objects and quantities in that row. Rows 3 and 4 give estimates of the quantity of each arrestin in the whole cone (column 2), or in its major subcellular compartments (OS, IS, cell body, axon, synaptic pedicle). In column 2, the total quantity for the entire cell is given in absolute units, while for the subcellular compartments the values given are fractions of the total. The data represent the average values extracted from 21 cones from cryosections of 3 mice. The volumetric quantities were extracted from LUMIj-Alexa555 fluorescence of cones with the 3D “cookie cutting” method, as illustrated in Figure 3.

[b]These volumes are distorted to higher values in part by the small size of the imaged objects relative to the microscope point-spread function; thus, EM data (Carter-Dawson & LaVail, 1979) leads to a cone OS envelope volume estimate of 14 μm^3, while our results yield the OS volume estimate $0.05 \times 950\ \mu m^3 = 47\ \mu m^3$; adjusted for this 3-fold over estimate, and for the ~ 2-fold ratio of OS water space to OS volume, the concentrations in the dark adapted cone OS would be about 6-fold higher than those given in the table.

Table 2

Physiological Properties of Cones of WT, *Arr4* $^{-/-}$, *Arr1* $^{-/-}$ and *Arr*-DKO Mice

Genotype, cell type **(no. of cells*)**	***Parameter*** ***Unit***	R_{max} **pA**	$\tilde{S}_F$ **ΔR%/(photons μm^{-2})**	A **(s^{-2})**	t_{peak}* **(ms)**	τ_D **(ms)**	$I_{½}$ **photons μm^{-2}s^{-1}**	$I'_{½}$ **photons μm^{-2}s^{-1}**
WT (n=29; 17)		7 ± 1	0.021 ±0.003	4.7 ± 0.6	69 ± 3	63 ± 5	(2.2 ± 0.4) × 10^5	(1.5 ± 0.3) × 10^5
Arr4$^{-/-}$ (n=11; 8)		7 ± 1	0.025 ± 0.006	6.7 ± 1.8	66 ± 4	84 ± 12	(1.6 ± 0.3) × 10^5	(1.0 ± 0.2) × 10^5
Arr1$^{-/-}$ (n=10; 6)		10 ± 3	0.033 ± 0.006	7.0 ± 1.2	65 ± 4	85 ± 12	(1.1 ± 0.3) × 10^5	(0.8 ± 0.2) × 10^5
Arr-DKO (n=18; 10)		9 ± 2	0.033 ± 0.007	6.9 ± 1.0	64 ± 2	NA	(0.8 ± 0.2) × 10^5	(0.6 ± 0.1) × 10^5

Column 1 gives the genotypes of the mice and numbers of cones of each genotype from which recordings were made (*the value of n after the semicolon gives the number from which step-response families were recorded). Columns 3–9 present parameters of the cells whose type is identified in the first column, as follows: R_{max} the saturating amplitude of the light response, $\tilde{S}_F$ the sensitivity of the normalized dim flash response, specified as percent of the saturating response per (photon μm^{-2}), A the amplification constant (Pugh and Lamb, 1993), t_{peak} the time to peak of the dim-flash response and τ_D the dominant recovery time constant (cf. Fig. 4). $I_{½}$ is the half-saturating step intensity, uncorrected for pigment depletion, and $I'_{½}$ the value obtained when pigment depletion is included (Fig 7). Error terms are ± 2 s.e.m. The sensitivity of S-dominant cones was measured with 361 nm flashes.

(*The time to peak has not been adjusted for the delay caused by the analog filtering of the recordings with the 8-pole, 20 Hz bandwidth filter used; measurements show this delay to be ~ 21 ms.). For estimating the amplification constant, an outer segment volume of 14 μm^3 and collecting area of 0.2 μm^2 at 360 nm was assumed for the S-dominant cones of all genotypes (Nikonov et al., 2006). One-way ANOVA's were performed to test the null hypothesis of no-difference between genotypes in each response parameter: significant differences exist between $\tilde{S}_F$, A, τ_D (WT, *Arr4*$^{-/-}$, *Arr1*$^{-/-}$ only), and $I'_{½}$ with $p < 0.002$, 0.001, 10^{-6}, 2×10^{-5}, respectively; there were no significant differences amongst genotypes in R_{max} and t_{peak}.